Supplemental figure legends:

Figure S1. Plot of the fluorescence ratio obtained by exciting Fura2 at 700 and 780 nm. Fura2 (100 μM) was loaded into SNc DA neurons in an ex vivo brain slice with the patch electrode. The excitation ratio (normalized to the initial excitation ratio of ionomycin at -90 mV, $R_{I\text{-}90}$), indicating a change in intracellular [Ca^{2+}], increased only at holding potentials above -60 mV (black traces). Superfusion with a solution lacking Ca^{2+} and containing EGTA (1.6 mM) and ionomycin (1 μM) to open pores in the outer cell membrane led to a stable excitation ratio that was independent of membrane voltage (red traces) and similar that obtained in physiological Ca^{2+} at membrane potentials below -60 mV; this demonstrates that intracellular [Ca^{2+}] was nominally zero (< 20 nM) at very negative membrane potentials. Average data from different cells in which the experiment was done are shade coded (thin lines). The average of 4 cells is presented in bold.

Figure S2. Fura2 recordings from pacemaking SNc DA neurons in *ex vivo* brain slices. A. Fura2 fluorescence measurements (with 780 nm excitation) from a SNc DA neuron in an ex vivo brain slice. The neuron was held at -90 mV in voltage clamp to pull the intracellular [Ca^{2+}] near zero. The fluorescence at this membrane potential was taken as f_{max}; it was taken at the site of the line scan prior to the measurements in current clamp while the cells were pacemaking; that is, f_{max} was measured for each trace or current clamp record just 20 sec before was acquired. **C.** The equation used to calculate [Ca^{2+}] from the Fura2 measurements using 780 nm excitation. Estimates of K_D and R_f used in the calculations are given in Methods. **D.** [Ca^{2+}] calculated from Fura2 measurements in **B**; visual definitions of peak, average and area are shown. **E.** Examples of [Ca^{2+}] estimates at a distal dendritic location at two different time points, 20-25 and 40-45 min after the break-in in to the cell **F.** The dendritic [Ca^{2+}] estimates are overlaid showing that the amplitude and kinetics of the

signals were stable. **G.** SNc DA distal dendrites have higher [Ca^{2+}] than proximal dendrites. Box plots summarizing peak, average (from historical control in figure 2**B**, **C**) and area of [Ca^{2+}] estimates from proximal and distal dendrites. Sample sizes for peak and average were 28 neurons from 23 mice for proximal and 31 neurons from 22 mice for distal dendrites. Sample sizes for area were 6 neurons from 6 mice for proximal and 8 neurons from 8 mice for distal dendrites. Each of these parameters was positively correlated with the others. Data were analyzed using one-tailed Mann-Whitney test. *P < 0.05.

Figure S3. [Ca^{2+}] increased with the frequency in both the proximal and distal dendrites. Box plots summarizing [Ca^{2+}] estimates in SNc DA neurons spiking at 0.5 Hz to 2 Hz, each frequency is grouped with its frequency ± 0.25 Hz. (1Hz data is from historical control in figure **2B, C**). Sample sizes for proximal dendrite were 17 neurons from 15 mice for 0.5 Hz, 28 neurons from 23 mice for 1 Hz, 19 neurons from 17 mice for 1.5 Hz, and 10 neurons from 10 mice for 2 Hz. For the distal dendrites, sample sizes were 22 neurons from 17 mice for 0.5 Hz, 31 neurons from 22 mice for 1 Hz, 20 neurons from 15 mice for 1.5 Hz, and 12 neurons from 10 mice for 2 Hz. Data were analyzed using one-tailed Mann-Whitney test. *P < 0.05.

Figure S4. Estimates of peak [Ca^{2+}] were not significantly different when using the low affinity Ca^{2+} dye bis-Fura2. A. Somatic whole-cell recordings from two SNc DA neurons in pacemaking mode; one was loaded with Fura2 (100 μM), the other with bis-Fura2 (100 μM). At the bottom, the fluorescence measurements from the two dyes in distal dendrites are shown. **B**. Box plots showing distal dendritic peak [Ca^{2+}] using bis-Fura2 (n = 7 neurons from 7 mice) were not substantially different from those with Fura2 (n = 31 neurons from 22 mice, from historical control in figure **2C**). Data were analyzed using one-tailed Mann-Whitney test. *P < 0.05.

Figure S5. Oscillations in cytosolic Ca^{2+} were significantly smaller in SNc DA neurons from immature mice. Box plots summarizing estimates of peak and average [Ca^{2+}] in proximal dendrites (A) and distal dendrites (B) of immature (P5-P10) and juvenile (P25-P35, from historical controls in figure 2B,C) SNc DA neurons. Sample sizes for proximal (A) dendrites were 28 neurons from 23 juvenile mice and 7 neurons from 3 immature mice, and for distal (B) dendrites 31 neurons from 22 juvenile mice and 8 neurons from 6 immature mice. Data were analyzed using one-tailed Mann-Whitney test. *P < 0.05.

Figure S6. Oscillations in cytosolic Ca^{2+} were significantly smaller in VTA DA neurons. Box plots summarizing the peak and average [Ca^{2+}] in proximal dendrites (**A**) and distal dendrites (**B**) of VTA and SNc neurons (from historical controls in figure **2B, C**). Sample sizes for proximal dendrites (**A**) were as follow: n = 28 SNc DA neurons from 23 mice and n = 9 VTA DA neurons from 3 mice. Sample sizes for distal dendrites (**B**) were as follow: n = 31 SNc DA neurons from 22 mice and n = 8 VTA DA neurons from 3 mice. Data were analyzed using one-tailed Mann-Whitney test. *P < 0.05.

Figure S7. Dendritic Ca^{2+} oscillation was largely unaffected by failure of the somatic spike. A. Upper panel showing somatic recordings from a P25 pacemaking SNc DA neuron; lower panel showing distal dendritic Ca^{2+} oscillations in these neurons. Dashed line indicates the peak [Ca^{2+}] during the episode. **B**. Box plots summarizing the percent change in the peak [Ca^{2+}] when a spike failed relative to the average of neighboring peaks associated with spikes. Sample size was n = 9 neurons (2 at proximal dendrites and 7 at distal dendrites) from 6 mice.

Figure S8. Chronic administration of isradipine didn't change open field behavior. A.

Representative movement tracks of an individual mouse over a 5-minute testing session; left is data from a control mouse, right is from an isradipine treated (7 days) mouse. **B**. Box plots summarizing data gathered from control (black box plots) and isradipine (green box plots) treated mice in total distance travelled, time spent in corners and time spent in the center. There were 9 mice in each group. Data were analyzed using one-tailed Mann-Whitney test. *P < 0.05**.**

Figure S9. Plasma isradipine concentration was similar following chronic treatment with pumps or pellets. A. Box plots summarizing the isradipine concentration in mice plasma after 7-10 days treatment with either pellets or pumps. For both, isradipine dose was 3mg/kg/day. There were 10 mice implanted with pellets and 6 mice implanted with pumps. Data were analyzed using two-tailed Mann-Whitney test; P = 0.692. **B.** Isradipine plasma concentration achieved in mice was within the range achieved in humans. Maximal plasma isradipine concentration from Park et al. (blue markers; T_{max} = 4 hrs for oral administration of single 5mg sustained-release isradipine) and Johnson et al. (red markers; T_{max} = 2 hrs for immediate release of 15 mg isradipine). Dotted line shows the median plasma concentration achieved in our study. Data were analyzed using one-tailed Mann-Whitney test. *P < 0.05**.**

Figure S10. Omission of isradipine from the bath had no significant effect on measured Ca^{2+} transients within 3-4 hours of sacrifice following chronic (7-10 days) isradipine administration. **A**. Box plots summarizing peak and average [Ca^{2+}] in proximal dendrites of SNc DA neurons in control condition (from historical controls in figure **2B**), after chronic isradipine treatment with osmotic minipumps (from historical chronic isradipine treatment in figure **4E**), and after 3 hours of washing in isradipine-free ACSF. Sample sizes were as follow: for control group n = 28 neurons from 23 mice, for chronic isradipine-treated group n = 5 neurons from 5 mice, for >3 hours washout after chronic isradipine-treated group n = 7

neurons from 3 mice. **B**. Box plots summarizing peak and average [Ca^{2+}] in distal dendrites in conditions same as in **A**. (control from figure **2B** and chronic isradipine treatment from figure **4F**) Sample sizes were: for the control group n = 31 neurons from 22 mice, for chronic isradipine-treated group n = 8 neurons from 8 mice, for >3 hours washout after chronic isradipine-treated group n = 10 neurons from 3 mice. Data were analyzed using one-tailed Mann-Whitney test with Dunn's correction for multiple comparison. *P < 0.05.

Figure S11. Bath application of 10 nM isradipine reduced dendritic [Ca^{2+}] in SNc DA neurons. A. & **B**. Example traces of whole-cell somatic recordings from SNc DA neurons firing at 1 (**A**) & 2 (**B**) Hz and, at the bottom, distal dendritic Ca^{2+} transients obtained with Fura2. 10nM isradipine treatment (green traces) reduced dendritic Ca^{2+} oscillations. **C**. Box plots summarizing proximal dendritic peak and average [Ca^{2+}] measurements in control (from historical control in figure **2B**) and 10 nM isradipine treated conditions. Sample sizes were: for the control group at 1 Hz n = 28 neurons from 23 mice, at 2 Hz n = 18 from 5 mice, for 10 nM isradipine treated group at 1 Hz n = 18 neurons from 5 mice, at 2 Hz n = 7 from 5 mice. **D**. Box plots summarizing distal dendritic peak and average [Ca^{2+}] measurements in control (from historical control in figure **2B**) and 10 nM isradipine treated conditions. Sample sizes were: for the control group at 1 Hz n = 31 neurons from 22 mice, at 2 Hz n = 15 from 13 mice, for 10 nM isradipine treated group at 1 Hz n = 14 neurons from 6 mice, at 2 Hz n = 5 from 2 mice. Data were analyzed using one-tailed Mann-Whitney test. *P < 0.05.

Figure S12. Three images of an SNc DA neuron used to estimate mitochondrial density in the cytoplasm. Left, image showing mito-roGFP fluorescence. Middle, image of red fluorescence in cytoplasm generated by a secondary antibody to a primary TH antibody. Right, DAPI fluorescence showing the nucleus. Scale bar=10 μm.

Figure S1 - Guzman et al.

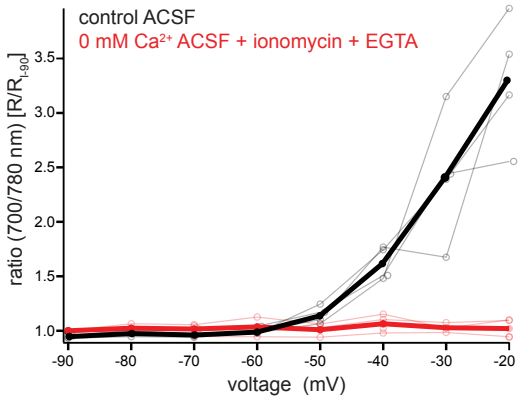

Figure S2 - Guzman et al.

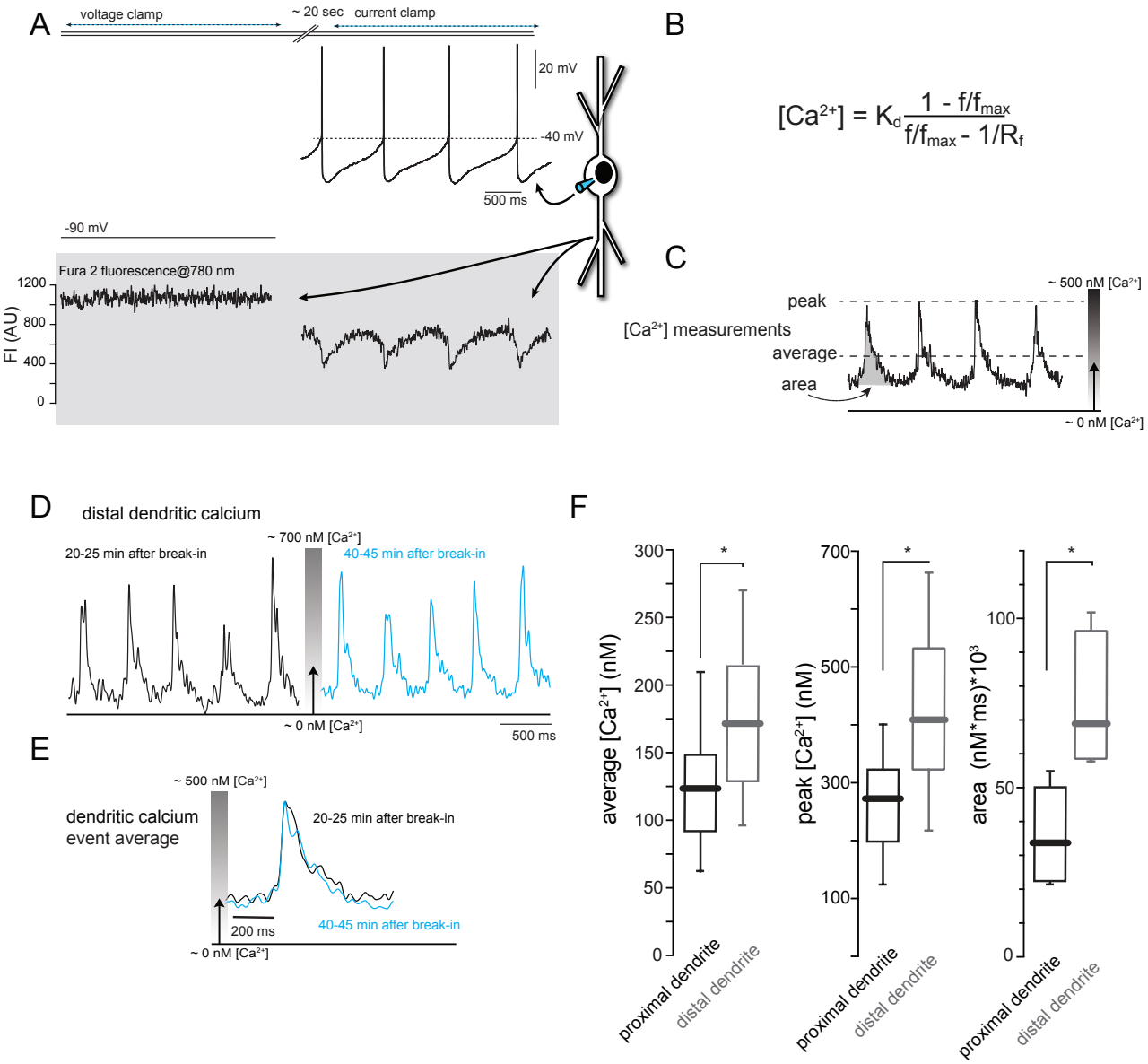

Figure S3 - Guzman et al.

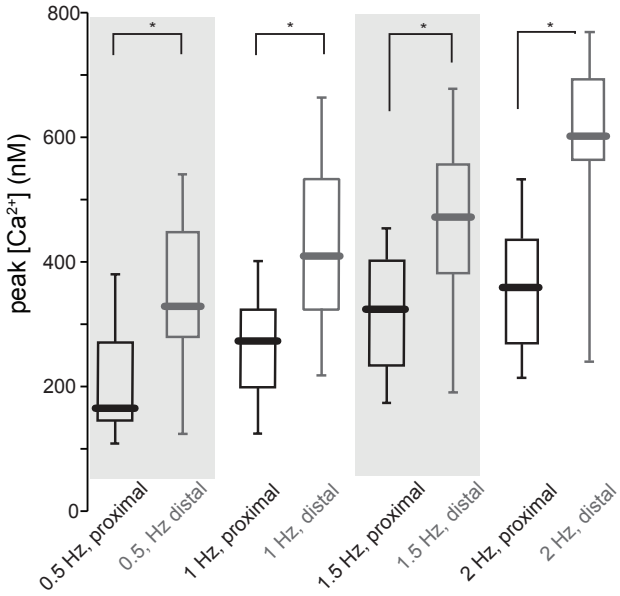

Figure S4 - Guzman et al.

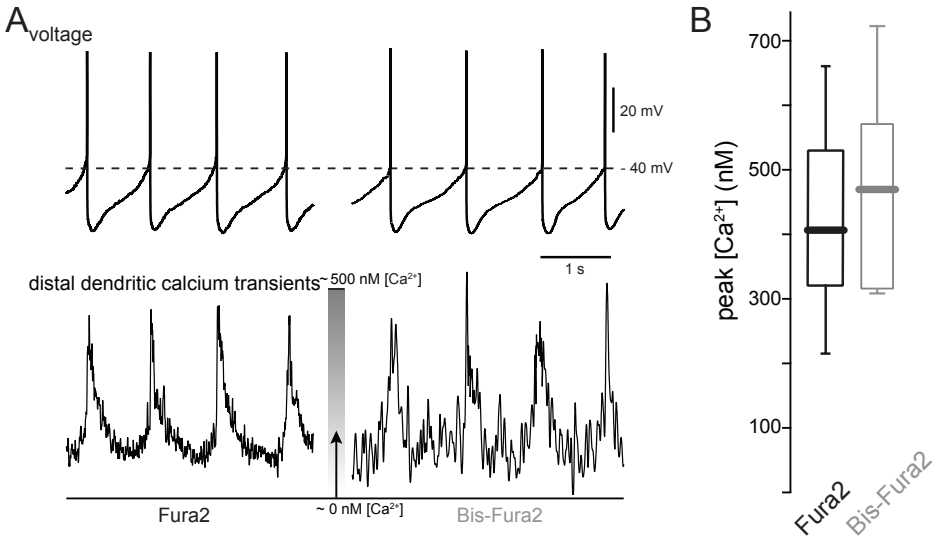

Figure S5 - Guzman et al.

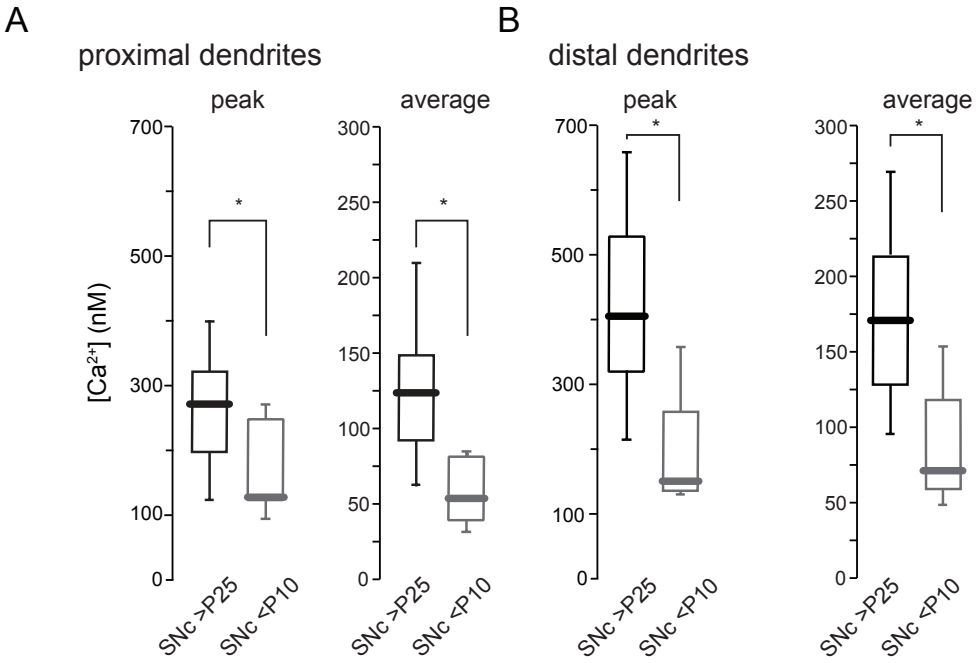

Figure S6 - Guzman et al.

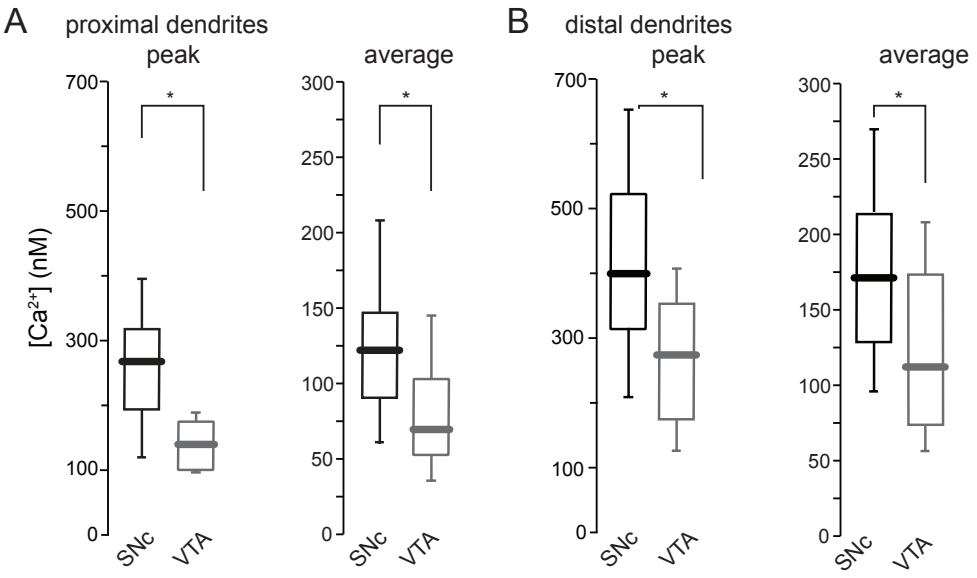

Figure S7 - Guzman et al.

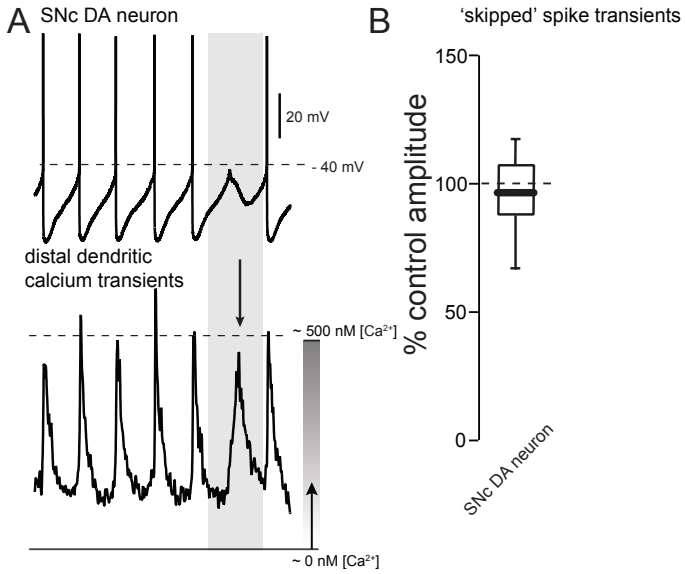

Figure S8 - Guzman et al.

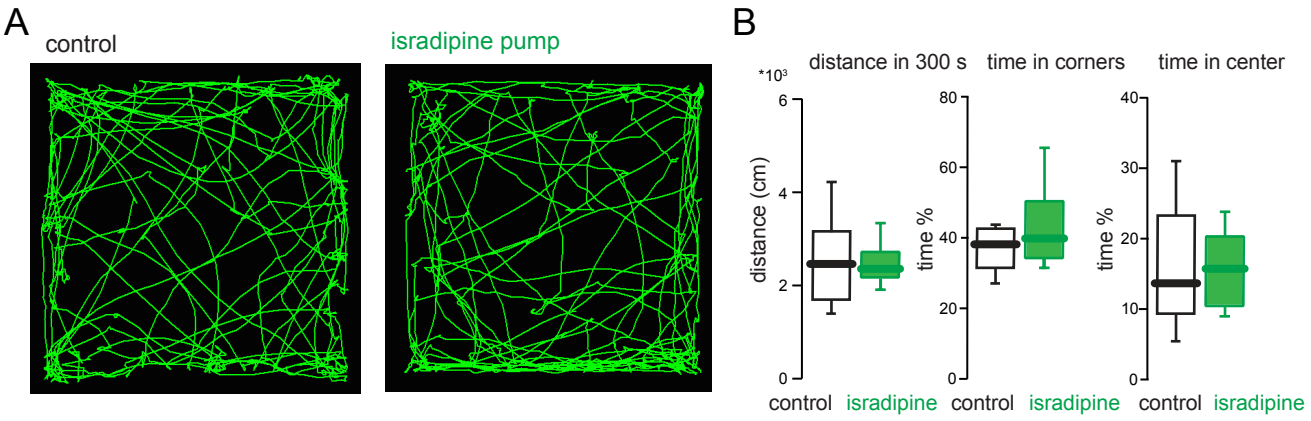

Figure S9 - Guzman et al.

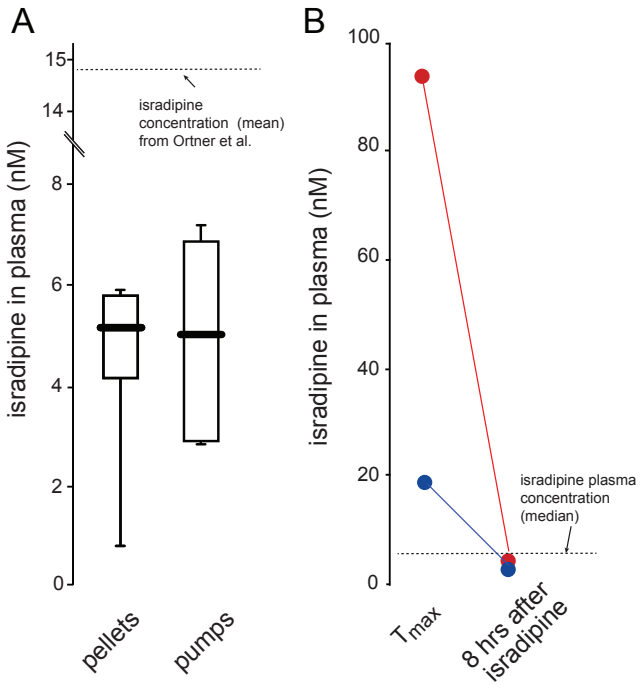

Figure S10 - Guzman et al.

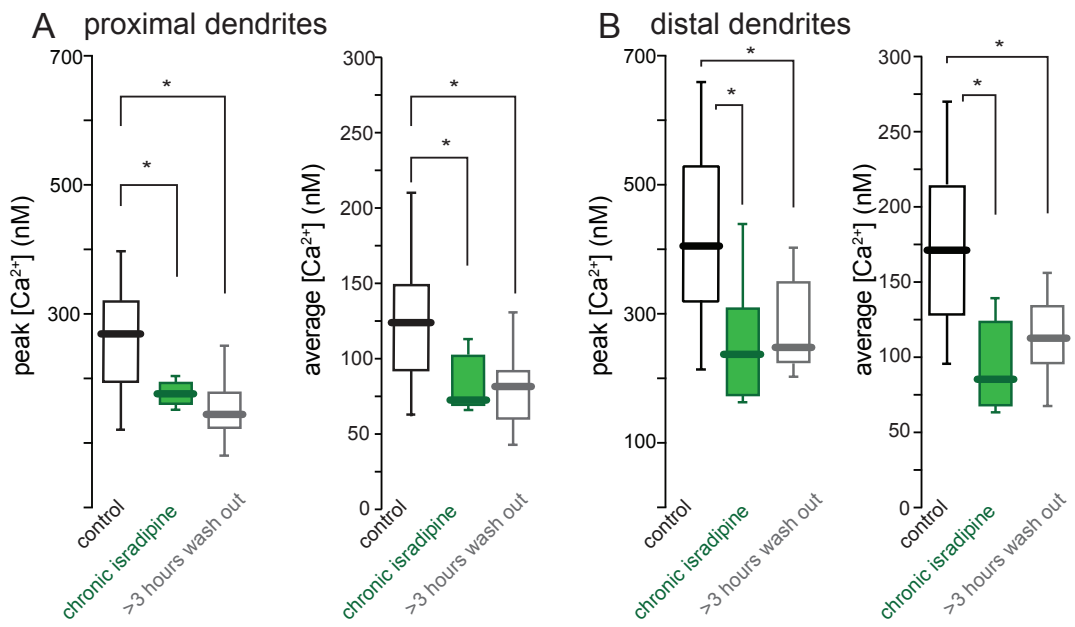

Figure S11 - Guzman et al.

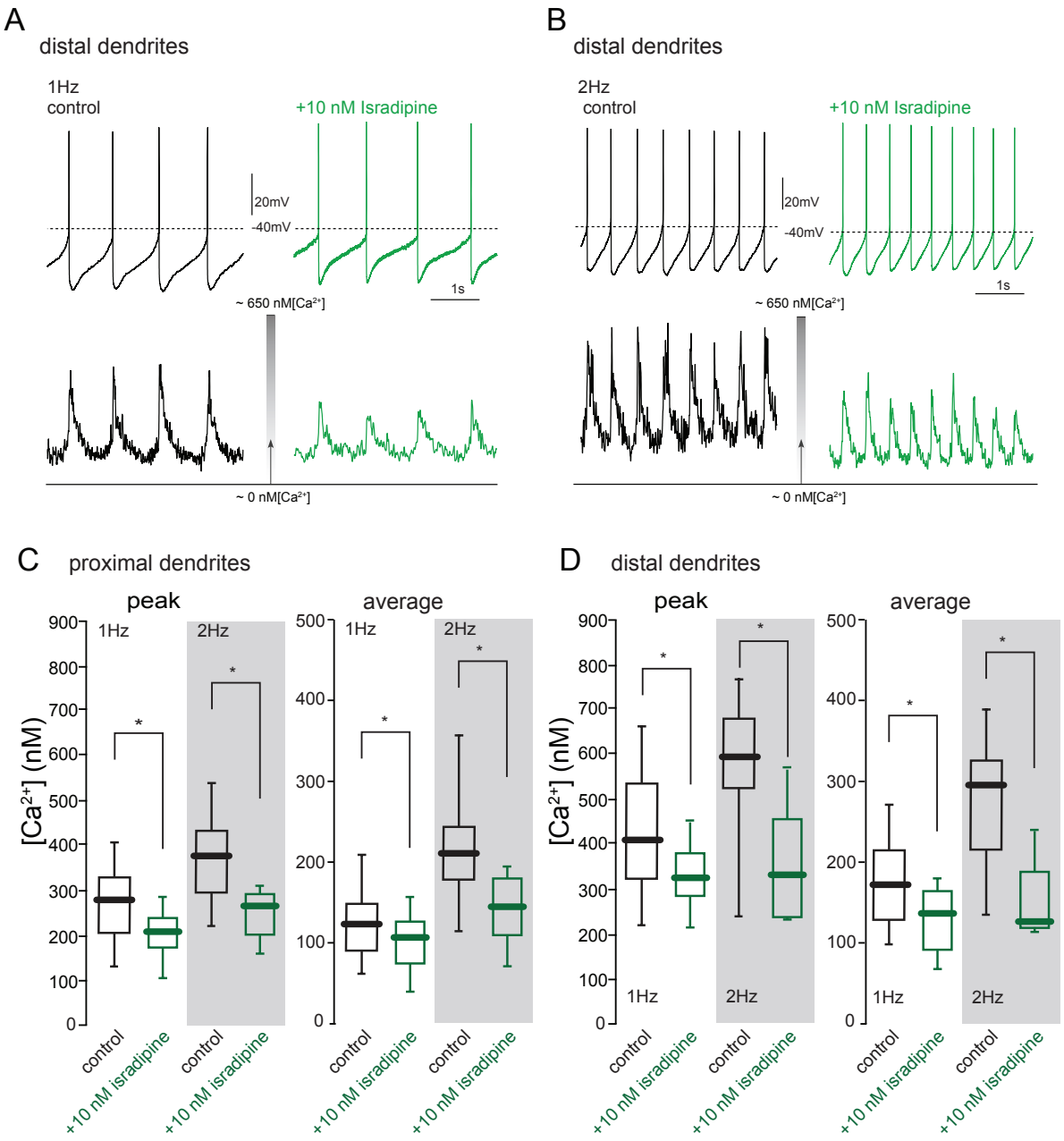

Figure S12 - Guzman et al.